Heliyon 10 (2024) e33802

Contents lists available at ScienceDirect

Heliyon

journal homepage: www.cell.com/heliyon

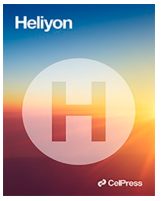

Research article

Isorhamnetin inhibits hypertrophic scar formation through TGF-β1/Smad and TGF-β1/CREB3L1 signaling pathways

Junzheng Wu [1], Yajuan Song [1], Jianzhang Wang [1], Tong Wang, Liu Yang, Yi Shi, Baoqiang Song [*], Zhou Yu [**]

Department of Plastic Surgery, Xijing Hospital, Fourth Military Medical University, Xi'an, China

ARTICLE INFO

Keywords:
Isorhamnetin
Hypertrophic scar
TGF-β1
CREB3L1
Smad2/3

ABSTRACT

Background: Hypertrophic scar (HS) is a common fibrotic skin disease that occurs secondary to burns or injuries. The activation of the TGF-β signaling pathway contributes immensely to HS formation. Isorhamnetin (ISO) is a type of flavonoid compound that exerts an antifibrotic effect via TGF-β signaling suppression. However, whether ISO can inhibit HS formation via TGF-β signaling is yet to be elucidated. This study aimed to examine the influence of ISO on HS pathogenesis and TGF-β signaling, especially the downstream molecules and networks of TGF-β signaling that facilitate HS formation.

Methods: Hypertrophic scar fibroblasts (HSFBs) were isolated from human HS tissues. The *in vitro* proliferation, migration, contractile ability, cell cycle, and apoptosis of HSFBs after ISO treatment were determined using cell viability assay, EdU staining, wound healing assay, collagen gel contraction assay, and flow cytometry. The expressions of genes and proteins involved in TGF-β signaling and its downstream molecules in ISO-treated HSFBs were determined using quantitative PCR (qPCR), immunofluorescence, and western blotting. *In vivo*, a rabbit HS model was established, and the effects of ISO on rabbit HS formation were investigated using histological analysis, immunohistochemical staining, and qPCR.

Results: In vitro studies indicated that ISO treatment suppressed the proliferation, migration, and contractile ability of HSFBs; attenuated the expressions of COL I, COL III, and α-SMA; and inhibited TGF-β1 signaling-induced activation of HSFBs by decreasing the levels of phosphorylated Smad2/3 and cleaved CREB3L1 in a dose-dependent manner. Furthermore, ISO augmented apoptosis and G2 phase cell cycle arrest of HSFBs by upregulating the expressions of the pro-apoptotic proteins Bax and cleaved caspase-3 and downregulating the expression of the anti-apoptotic protein Bcl-2. *In vivo* studies revealed that ISO ameliorated HS formation in the rabbit ear by lowering the scar elevation index, attenuating the collagen density, facilitating the regular arrangement of collagen fibers, and downregulating the expressions of TGF-β1, CREB3L1, COL I, COL III, and α-SMA.

Abbreviations: HS, hypertrophic scar; ISO, isorhamnetin; HSFBs, hypertrophic scar fibroblasts; NFBs, normal fibroblasts; RIP, regulated intramembrane proteolysis; ECM, extracellular matrix; CREB3L1, cAMP response element binding protein 3-like 1; TGF-β/Smad, transforming growth factor-β/Smad; PBS, phosphate-buffered saline; FBS, fetal bovine serum; PI, propidium Iodide; α-SMA, α-smooth muscle actin**smoothmuscle actin**; qPCR, quantitative polymerase chain reaction; GADPH, glyceraldehyde 3-phosphate dehydrogenase; PPI, protein–protein interaction.

* Corresponding author.
** Corresponding author.
E-mail addresses: songbq2012@163.com (B. Song), yz20080512@163.com (Z. Yu).
[1] These authors contributed equally to this work.

https://doi.org/10.1016/j.heliyon.2024.e33802
Received 12 October 2023; Received in revised form 26 June 2024; Accepted 27 June 2024
Available online 29 June 2024

Conclusions: ISO suppressed HS pathogenesis by dampening TGF-β1/Smad and TGF-β1/CREB3L1 signaling pathways, which suggests that it may serve as a candidate inhibitor of TGF-β1 signaling and a promising anti-HS drug with a high therapeutic potential.

1. Introduction

Hypertrophic scar (HS) is a dermal fibroproliferative disorder characterized by the abnormal proliferation of fibroblasts and the excessive deposition of extracellular matrix (ECM) [1]. HS can be caused by deep skin trauma, surgery, or burns, and clinically, this condition involves features such as redness, hard texture, and varying degrees of pruritus. Patients with HS often endure substantial physical and mental pain, which affects their quality of life [2]. Presently, local drug sealing, pressure therapy, surgery, radiation, laser therapy, etc., are used for HS treatment. However, these methods are associated with various side effects, time-consuming, and accompanied by pain [3]. Therefore, an efficient and safe drug is urgently needed for HS treatment.

During HS formation, the transforming growth factor-β/Smad (TGF-β/Smad) pathway plays an important role by stimulating fibroblast proliferation, migration, and activation and enhancing the synthesis and deposition of ECM proteins, such as type I and type III collagens, thus facilitating abnormal collagen degradation and scar formation [4,5]. Therefore, the TGF-β/Smad signaling has become a potential therapeutic target for HS. Experimentally, TGF-β–mediated gene transcription is highly dependent on the activation of Smad2/3. However, the level of phosphorylated Smad2/3 decreases within hours even in the persistent presence of TGF-β1 [6]. On the contrary, the collagen-stimulating effect of TGF-β1 can last for days [7], which indicates that it can promote tissue fibrosis even in the absence of phosphorylated Smad2/3. These findings suggest that TGF-β1 activates the downstream genes involved in ECM synthesis and deposition independent of Smad2/3. Nonetheless, the downstream genes that transmit the collagen-stimulating signal of TGF-β1 are yet to be investigated. In addition, a study has shown that cAMP response element binding protein 3-like 1 (CREB3L1) acts as a downstream molecule of TGF-β1 and is involved in the assembly of the collagen-containing ECM. More importantly, under TGF-β1 stimulation, CREB3L1 can be cleaved into a transcription factor via regulated intramembrane proteolysis (RIP), thus transcriptionally regulating the expressions of genes related to ECM synthesis [8]. Thus, both TGF-β/Smad and TGF-β/CREB3L1 signaling pathways might contribute to HS formation, and exploring drugs that target these pathways may be conducive to HS treatment.

Isorhamnetin (ISO, $C_{16}H_{12}O_7$, Fig. 1A) is a type of flavonoid compound that occurs in various types of plants, such as *Hippophae rhamnoides* L and *Ginkgo biloba* L. A previous study showed that ISO exhibits several biological activities, including anti-inflammatory, antioxidant, antitumor activity, and antifibrosis [9,10]. Liu et al. reported that ISO suppresses liver fibrosis by decreasing ECM deposition via TGF-β1/Smad3 and TGF-β1/p38 MAPK pathways [11]. In addition, Yang et al. confirmed that ISO improves carbon

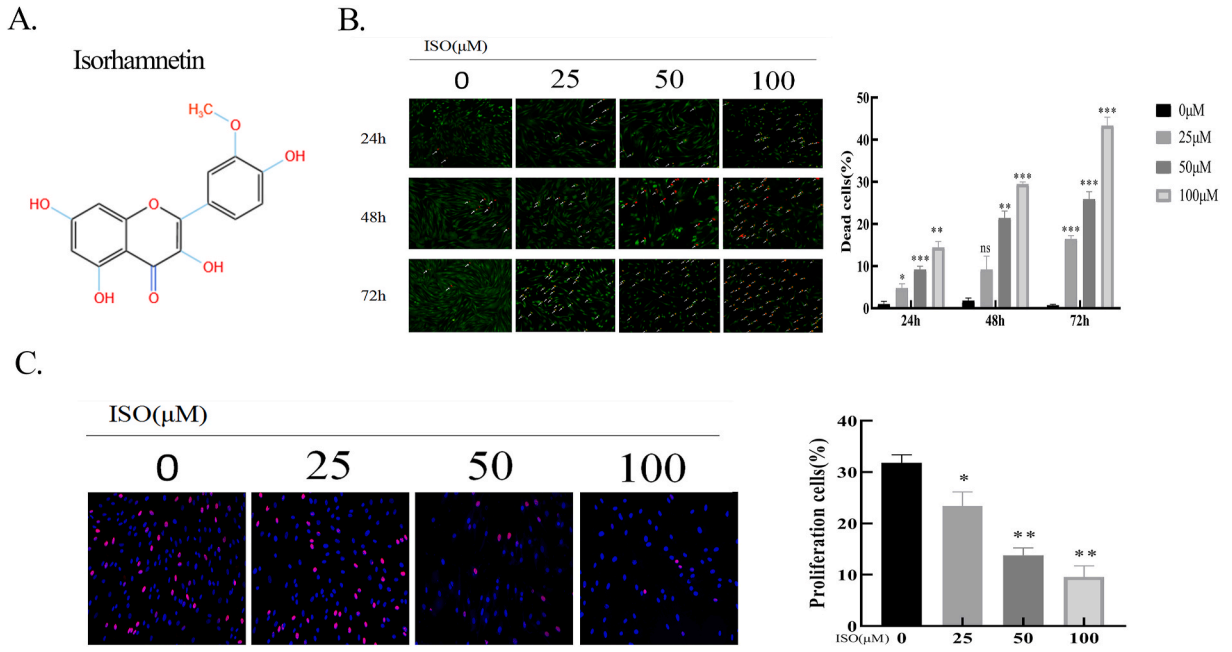

Fig. 1. ISO inhibited HSFBs proliferation. A. Chemical structure of ISO. B. Calcein-AM/PI double staining for cell viability of HSFBs after incubation with ISO (0, 25, 50, 100 μM) for 24, 48, and 72 h. Living cells are labeled by green fluorescence, while dead cells are labeled by red fluorescence. The quantification of the percentage of dead cells. C. EdU staining of HSFBs after treatment with ISO (0, 25, 50, 100 μM) for 48 h. Left panel: the representative images of Edu staining. Right panel: quantification of the percentage of EdU-positive cells. *p < 0.05, **p < 0.01, ***p < 0.001.

tetrachloride-4–induced liver fibrosis by inhibiting the TGF-β1/Smad pathway and alleviating oxidative stress [12]. Moreover, numerous studies have confirmed that TGF-β1 promotes HS formation [13–15]. Nevertheless, whether ISO can inhibit HS formation by suppressing TGF-β1/Smad and TGF-β1/CREB3L1 signaling is yet to be determined.

In this study, the effects of ISO on HS formation and the underlying mechanisms were investigated using various *in vitro* and *in vivo* experiments. The results signified that ISO could ameliorate HS formation by inhibiting TGF-β1/Smad and TGF-β1/CREB3L1 signaling pathways.

2. Materials and methods

2.1. Patient samples

Human hypertrophic scars tissues and normal skin tissues were obtained from patients receiving scar revision surgery at Xijing Hospital. This study was reviewed and approved by the Institutional Review Board of the Xijing Hospital. All studies were approved by the Institutional Review Board of the Xijing Hospital and were conducted in accordance with the principles of the Declaration of Helsinki.

2.2. Isolation and culture of human fibroblasts

For the isolation of hypertrophic scar fibroblasts (HSFBs) and normal fibroblasts (NFBs), tissue samples were washed thrice with phosphate-buffered saline (PBS) containing penicillin (100 U/mL) and streptomycin (0.1 mg/mL) and then trimmed to remove subcutaneous adipose tissue. Subsequently, the remaining tissues were minced into small pieces and placed in Dulbecco's modified Eagle medium (Hyclone Inc., USA) containing 10 % fetal bovine serum (FBS, Gibco Life Technologies, USA). All cultures were maintained in a 5 % CO_2 incubator at 37 °C. The cells were passaged close to confluence, and cultured fibroblasts that had been passaged 4–8 times were used in this study.

2.3. Cell viability assay

Cell viability was detected using a Calcein-AM/Propidium Iodide (PI) Double Stain Kit (Solarbio, Beijing, China). HSFBs (6×10^4/well) were seeded into 24-well plates. After overnight culturing, the cells were treated with different concentrations of ISO (0, 25, 50, and 100 μM) for 48 h. According to the manufacturer's protocol, the cells were incubated in the kit buffer containing 2 μM calcein AM (living cells produce green fluorescence) and 8 μM PI (dead cells produce red fluorescence) for 1 h. The fluorescence images were captured using an inverted fluorescence microscope (ECLIPSE Ni-E, Niko, Tokyo, Japan).

2.4. Cell proliferation assay

The cell proliferation assay was performed using BeyoClick™ EdU Cell Proliferation Kit with Alexa Fluor 488 (Beyotime, China). In brief, HSFBs (2×10^4 cells/well) were seeded in 24-well plates and cultured in a medium containing different concentrations of ISO (0, 25, 50, and 100 μM) for 48 h. Subsequently, the cells were incubated with EdU staining buffer for 4 h, fixed with 4 % paraformaldehyde for 15 min at room temperature, and permeabilized using PBS containing 0.3 % Triton-X100 for 15 min. The cells were then incubated with the click reaction solution at room temperature for 30 min in the dark and stained with Hoechst 33342 for 10 min. The stained cells were finally examined using a fluorescence microscope (ECLIPSE Ni-E, Niko, Tokyo, Japan).

2.5. Wound healing assay

HSFBs were seeded in a six-well plate at a density of 3×10^5 cells per well, and the cell monolayer was scratched using a sterile 200 μL pipette tip. The cells were treated with 2 μg/mL mitomycin C for 2 h, after which the culture wells were washed thrice with PBS and the cells were treated with different concentrations of ISO. The wound areas were then photographed and quantified with the ImageJ software (Version 1.52a, NIH, USA).

2.6. Collagen gel contraction assay

The effects of ISO on fibroblast-mediated collagen gel contraction were determined using the CytoSelect 24-well Cell Contraction Assay Kit (Cell Biolabs, San Diego, CA) according to the manufacturer's instructions. Fibroblasts were harvested and resuspended in the collagen solution at 2×10^7 cells/mL. Later, 0.5 mL of the solution was added to each well of the 24-well plate, and incubated at 37 °C for 1 h to allow collagen polymerization. Subsequently, 1 mL medium containing 10 % FBS was added (with/without ISO) to each well and replaced every 24 h. Wells that did not contain any cells in the collagen solution served as the control. Gel contraction was determined by measuring the areas of the gel surface after 24, 48, and 72 h. Areas of collagen gel contraction were measured and quantified using the ImageJ software (Version 1.52a, NIH, USA).

2.7. Cell cycle analysis

HSFBs were plated in six-well plates at a density of 5×10^5 cells/well and cultured in a medium containing various concentrations of ISO (0, 25, 50, and 100 μM) for 48 h. The cells were subsequently collected, washed, and resuspended in PBS and fixed using 70 % ice-cold ethanol for 24 h at 4 °C. The fixed samples were stained using the Cell Cycle and Apoptosis Analysis Kit (US Everbright Inc., USA) according to the manufacturer's instructions. The cells were centrifuged to remove the ethanol and incubated in the cell cycle staining solution containing PI in the dark at room temperature for 30 min. The cell cycle was then analyzed using flow cytometry.

2.8. Apoptosis detection

Cell apoptosis was measured with the Annexin V-FITC Apoptosis Detection Kit (Solarbio, Beijing, China) according to the manufacturer's guidelines. Briefly, HSFBs (3×10^6/well) were seeded in 12-well plates. After culturing them for 24 h, the cells were treated with different concentrations of ISO (0, 25, 50, and 100 μM) for 48 h. The cells were then trypsinized and transferred into 1.5 mL centrifuge tubes and 100 μL of binding buffer was added to each tube, followed by the addition of 5 μL each of Annexin V-FITC and PI. The cells were incubated for 15 min in the dark at room temperature. Finally, they were analyzed using flow cytometry (FACS Calibur, BD), and the results were scrutinized using the FlowJo 7.6.2 software (Tree Star Inc., USA).

2.9. Immunofluorescence

HSFBs were seeded in 24-well plates (3×10^5/well) and allowed to grow into a monolayer. Media containing varying concentrations of ISO (0, 25, 50, and 100 μM) were added to each well for 48 h. The cells were washed with PBS thrice, fixed with 4 % paraformaldehyde for 10 min, and incubated with anti-α-SMA antibody (Proteintech, China, 1:500) overnight at 4 °C. After washing with PBS, the cells were incubated with anti-rabbit IgG-AlexaFluor 488 (Absin, China, 1:500) under dark conditions at room temperature for 1 h. The nuclei were stained with DAPI, and the images were viewed under a fluorescence microscope (ECLIPSE Ni-E, Niko, Tokyo, Japan) and analyzed using the ImageJ software (Version 1.52a, NIH, USA).

2.10. Western blotting

HSFBs (6×10^5 cells/well) were seeded in 12-well plates and cultured in media containing varying concentrations of ISO (0, 25, 50, and 100 μM) for 48 h. After washing with cold PBS, RIPA lysis buffer with protease and phosphatase inhibitors was added to extract the total proteins. The protein concentration in each sample was measured using the BCA Protein Assay Kit (Beyotime). Equal amounts of proteins were separated using 7.5 % sodium dodecyl sulfate-polyacrylamide gel electrophoresis and transferred onto the polyvinylidene fluoride membranes. The membranes were blocked using PBS with Tween-20 containing 5 % bovine serum albumin at room temperature for 1 h. The membranes were then cut horizontally to detect the proteins of interest and incubated overnight at 4 °C with the following primary antibodies: α-SMA (Proteintech, 1:100), TGF-β1 (Proteintech, 1:1000), Smad2/3 (Cell Signaling, 1:1000), *p*-Smad2/3 (Cell Signaling, 1:1000), COL I (Proteintech, 1:1000), COL III (Proteintech, 1:1000), MMP2 (Proteintech, 1:1000), MMP9 (Proteintech, 1:1000), Bax (Proteintech, 1:1000), Bcl-2 (Proteintech, 1:1000), CREB3L1 (Proteintech, 1:1000), and Caspase 3 (Proteintech, 1:1000). On Day 2, the membrane was incubated with anti-rabbit HRP-labeled secondary antibody (Proteintech, 1:10000) for 2 h at room temperature. The blots were then imaged using a chemiluminescence imaging system, and the ImageJ software (Version 1.52a, NIH, USA) was used for densitometry. The protein levels were calculated based on the ratio of the corresponding protein and glyceraldehyde 3-phosphate dehydrogenase (GADPH).

2.11. Quantitative PCR

Quantitative polymerase chain reaction (qPCR) was applied to detect the mRNA expressions of genes (*α-SMA, TGF-β1, COLI, COL III,andCREB3L1*). Total RNA was extracted using the TRIzol reagent (Thermo Fisher Scientific, USA). After measuring the concentrations, 1 μg of total RNA was reverse-transcribed into cDNA using the Hifair® II 1st Strand cDNA Synthesis Kit (YEASEN, China) at 37 °C for 15 min. qPCR was performed using the CFX Connect™ Real-Time System (BIO-RAD, USA) and Hieff® PCR SYBR Green Mix (YEASEN). The primer sequences are listed in Table 1, and qPCR cycling was performed with denaturation at 95 °C for 30 s, and then, 95 °C for 5 s and 60 °C for 30 s (40 cycles). The mRNA levels were calculated using the $2^{-\Delta\Delta CT}$ formula after normalization to GADPH.

Table 1
The sequences of primers used in the study.

Gene	Forward Primer	Reverse Primer
COLIII	5′-TTCCTTTTGTTCTAATCTTGTCA-3′	5′-TAGCACCATTGAGACATTTTGA-3′
COLI	5′-TGAGCCAGCAGATTGAGAAC-3′	5′-CCAGTGTCCATGTCGCAGA-3′
TGF-β1	5′-AGGACGCCAACTTCTGCCT-3′	5′-AGGACCTTGCTGTACTGGGTGT-3′
α-SMA	5′-TTCTGCATACGGTCAGCAAT-3′	5′-CATCCATGAAACCACCTACA-3′
CREB3L1	5′-CACGCTTCCTCCCCAGTG-3′	5′-GCTTCATTTCCCAGCCATCC-3′
GAPDH	5′-GAACGGGAAACTCACTGGCAT-3′	5′-CCTTCTTGATGTCGTCATACTTAGC-3′

Table 2
The sequences of si-CREB3L1 used in the study.

Name	Sequences	Sequences
CREB3L1#1	5′-GGUGAACCAGUUCCUCAAA-3′	5′-UUUGAGGAACUGGUUCACC-3′
CREB3L1#2	5′-CAUUUACAUCUGAACAAAC-3′	5′-UUGUUCUCAGAUGUAAAUG-3′
CREB3L1#3	5′-GCUCCAGCAGCUGCAGAAA-3′	5′-UUUCUGCAGCUGCUGGAGC-3′

2.12. Cell transfection

CREB3L1 siRNA (si-CREB3L1) and siRNA NC (si-NC) were synthesized by Tsingke Biotechnology (Beijing, China). HSFBs in six-well plates were transfected with 20 nM CREB3L1 siRNA using the Lipofectamine 3000 reagent (Invitrogen, ThermoFisher Scientific, America) per the manufacturer's protocol. The siRNA sequences are listed in Table 2. The knockdown effects were assessed using western blotting.

2.13. Animal model

Eight male New Zealand white rabbits (8 weeks old) were housed in individual cages and maintained under a 12-h light/dark cycle with free access to food and water. All animal procedures were approved by the Animal Investigation Committee of the Institute of Biomedical Sciences, the Fourth Military Medical University. The rabbit ear model of cutaneous HS was prepared according to our previous published article [16]. Briefly, New Zealand white rabbits were anesthetized via the intravenous injection of 1 % (10 g/L) pentobarbital sodium at a dose of 40 mg/kg. The rabbit ears were disinfected with iodophor and shaved. Four full-thickness circular wounds of 1 cm were created on the ventral side of each ear using a biopsy punch of 1 cm diameter. The skin and the perichondrium in each wound were completely removed using a surgical blade, and the wounds were cleaned and exposed to air. Three weeks later, each wound on the left ear was injected subcutaneously with 50 μL of 0.1 % DMSO as a control. Conversely, each wound on the right ear was injected with 50 μL (100 μM/mL) of ISO every 3 days. After 35 days, scar tissues were collected from each group. One-half of the specimen tissues were fixed with 4 % paraformaldehyde solution for histological staining, and the other half was frozen in liquid nitrogen for qPCR.

2.14. Histology

Rabbit ear scar tissues were fixed with 4 % paraformaldehyde overnight, embedded in paraffin, and cut into 5–μm–thick sections. Then, the sections were stained with hematoxylin and eosin and Masson's trichrome staining.

2.15. Immunohistochemistry

For immunohistochemical staining, the sections were incubated overnight at 4 °C with primary antibodies against α-SMA diluted at 1:100. Subsequently, they were incubated with HRP-conjugated secondary antibody for 1 h at room temperature. The sections were visualized with a DAB Detection Kit and counterstained with hematoxylin. The images were then viewed under a light microscope (ECLIPSE Ti2, Niko, Tokyo, Japan)

2.16. Statistical analysis

The data were presented as the mean ± standard deviation. Statistical analyses were performed using student's t-test, one-way analysis of variance (ANOVA), or two-way ANOVA (GraphPad Prism 6.0). After one-way or two-way ANOVA, the post-hoc test (Tukey's test) was performed. A value of $P < 0.05$ was considered to indicate statistical significance.

3. Results

1. ISO inhibited HSFBs proliferation

Fibroblast proliferation is strongly implicated in HS formation [17]. To assess the effects of ISO on HSFBs proliferation, calcein-AM and PI staining were performed to identify the live and dead cells. As illustrated in Fig. 1B, compared with the control group, treatment with different concentrations of ISO (25, 50, and 100 μM) for varying periods (24, 48, or 72 h) resulted in a lower density of live cells (green) and a higher density of dead cells (red) in a dose- and time-dependent manner. Specifically, the effects of ISO treatment at different concentrations for 24 h on HSFBs viability were relatively mild, whereas 72 h treatment resulted in a high percentage of cell death. The cell death percentage of the 100 μM ISO-treated group was as high as 47.8 %. As an adequate percentage of live cells was required for subsequent experiments, 48 h was selected as the treatment time for further studies. Moreover, to visually assess the antiproliferative effect of ISO, an EdU incorporation assay was utilized to determine the proliferation cells. The findings indicated that ISO significantly inhibited HSFBs proliferation in a dose-dependent manner ($P < 0.05$) (Fig. 1C), which agreed with the results of the calcein-AM and PI staining assay.

2. ISO promoted HSFBs apoptosis and induced cell cycle arrest

The effects of ISO on HSFBs apoptosis were then evaluated. The results of flow cytometry showed that ISO induced HFSBs apoptosis as its concentration increased (Fig. 2A). Western blot findings revealed that when HSFBs were exposed to different concentrations of ISO, an increase in the expression of the proapoptotic protein Bax and a decrease in the expression of the antiapoptotic protein Bcl-2 were observed. Moreover, ISO increased the protein level of cleaved Caspase-3 and reduced the level of pro-Caspase-3 in HSFBs (Fig. 2B). These results demonstrated that ISO could induce HSFBs apoptosis in a dose-dependent manner. Apoptosis is often accompanied by cell cycle arrest [18]. Therefore, whether ISO could induce HSFBs cell cycle arrest was explored. As shown in Fig. 2C, upon stimulation by ISO, the proportion of cells in the G2 phase increased significantly and that of cells in the G1 phase decreased significantly. These findings assert that ISO promoted HSFBs apoptosis by inducing cell cycle arrest.

3. ISO suppressed HSFBs migration

Wound healing and transwell assays were performed to determine the effects of ISO on HSFB migration. As demonstrated in Fig. 3 A and B, compared with the control group (0 μM), ISO treatment decreased the horizontal migration of HSFBs, and considerable differences were noted in the 50 and 100 μM groups. The results of the wound healing assay were similar to those of the transwell assay. ISO inhibited the vertical migration of HSFBs in a dose-dependent manner (Fig. 3C and D). Furthermore, to validate the inhibitory

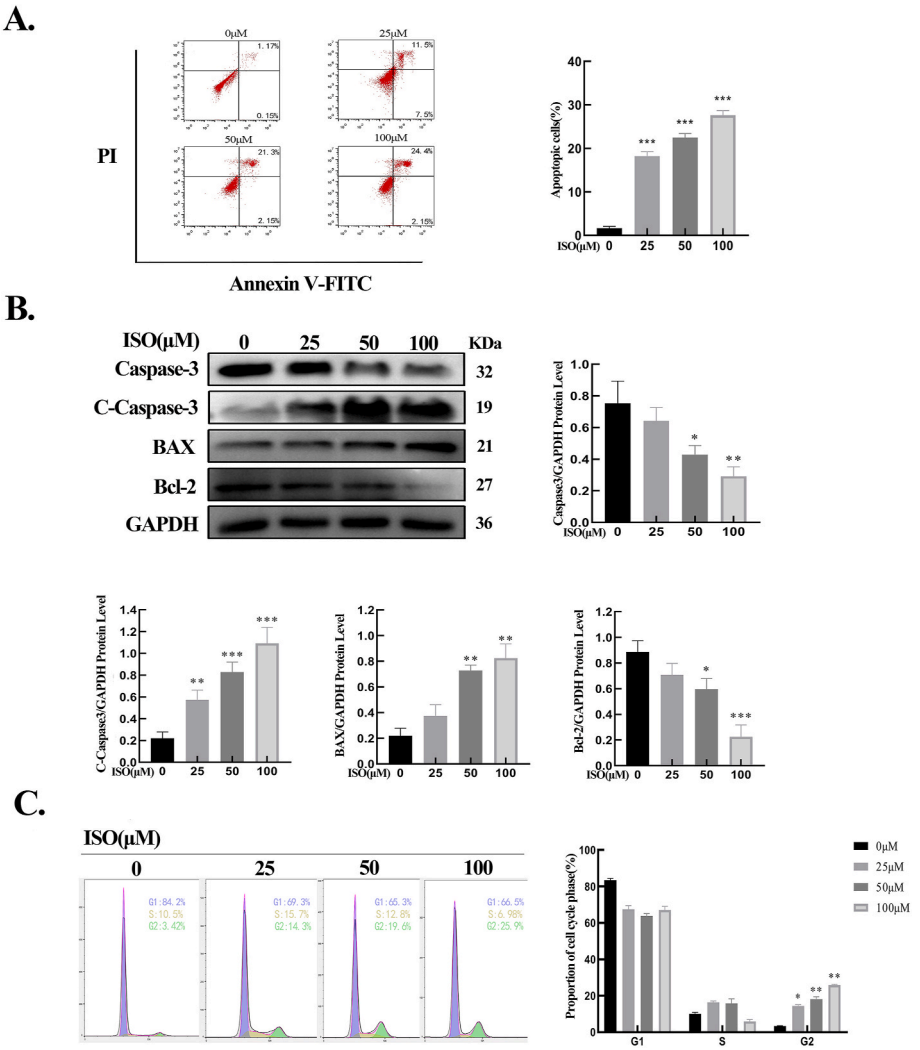

Fig. 2. ISO promoted HSFBs apoptosis and induced cell cycle arrest. A. The flow cytometry results and quantification of the apoptotic cells of HSFBs. B. The expressions of apoptotic proteins in HSFBs and quantification of the apoptotic protein levels normalized to GAPDH. C. Flow cytometry results and quantification of HSFBs cell cycles. All assays were conducted with HSFBs after treatment with ISO of different concentrations (0, 25, 50, 100 μM) for 48 h. *$p < 0.05$, **$p < 0.01$, ***$p < 0.001$.

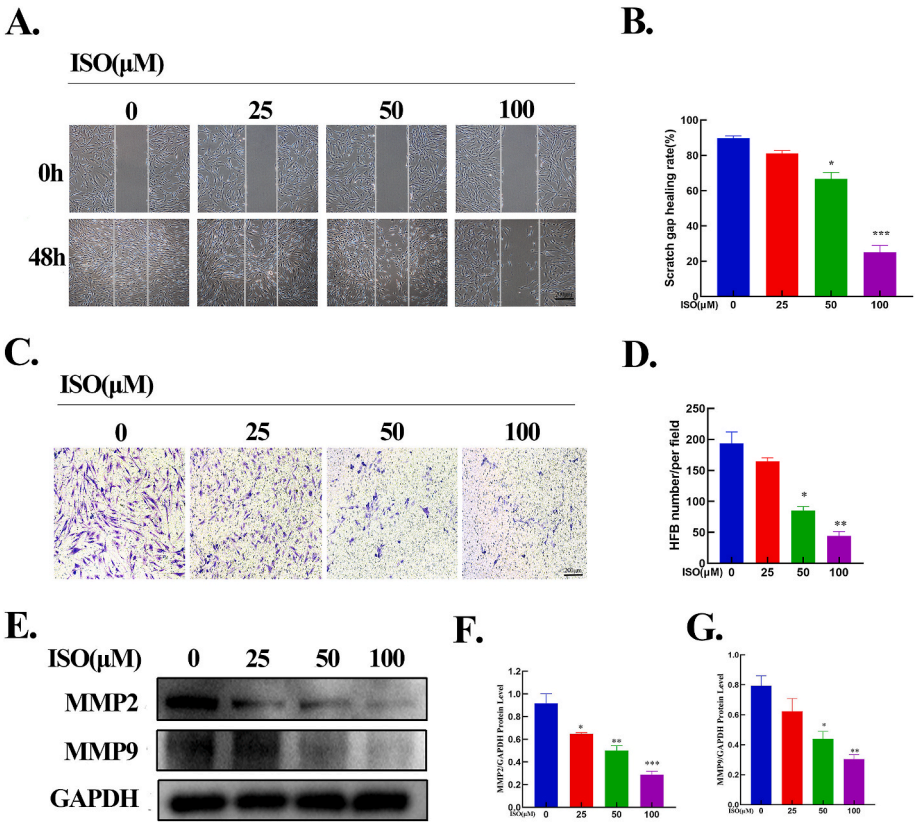

Fig. 3. ISO suppressed HSFBs migration. A-B. Images and quantitative results of the wound-healing assay. ISO attenuated the horizontal migration of HFSBs with an increase in ISO concentrations. Dotted lines indicate the scratch areas. C-D. Images and quantitative results of the transwell assay. E-G. Western blotting and quantification of MMP2 and MMP9 normalized to GAPDH. All assays were conducted with HSFBs after treatment with ISO of different concentrations (0, 25, 50, 100 μM) for 48 h. *p < 0.05, **p < 0.01, ***p < 0.001.

effects of ISO on the invasive capability of HSFBs, the protein levels of MMP-2 and MMP-9 were assessed. The results signified that ISO reduced the protein expressions of MMP-2 and MMP-9 as its concentration increased (Fig. 3E-G). These results confirm that ISO significantly suppressed the horizontal and vertical migrations of HSFBs.

4. ISO dose-dependently inhibited fibroblast activation and collagen expression

To explore the effects of ISO on HSFB-mediated contraction of ECM, a collagen gel contraction assay was performed. When compared with the control group (0 μM), ISO treatment attenuated the areas of gel contraction as the drug concentration increased (Fig. 4A). Furthermore, the effect of ISO on α-SMA expression was investigated, which showed that ISO decreased the expression dose-dependently (Fig. 4B, C). Subsequently, the effect of ISO on fibroblast-to-myofibroblast transition was evaluated using NFBs stimulated with TGF-β1 (10 ng/mL). The results illustrated that ISO inhibited the protein expression of α-SMA induced by TGF-β1 in a dose-dependent manner (Fig. 4B, C). Finally, the expressions of COL I and COL III in HSFBs were detected, which indicated that ISO dose-dependently downregulated these protein levels (Fig. 4D). Thus, ISO dose-dependently inhibited fibroblast activation and collagen expression.

5. Network pharmacology analysis

Considering the inhibitory effects of ISO on HSFBs, network pharmacology analysis was used to identify the potential targets of ISO for HS. By retrieving the TCMSP database and standardization using the UniProt database, a total of 45 potential targets of ISO were retrieved (Fig. 5A). Potential targets related to ISO were searched in two databases, as a result of which 1231 targets were obtained from the GeneCards database and 40 targets from the OMIM database. After combining the two databases and deleting the repeated targets, a total of 1256 HS-related targets were obtained. To identify the intersection of ISO and HS target genes, the Venny online mapping platform was used. As depicted in Fig. 5B, 16 intersection targets of ISO and HS were acquired. These targets were imported into the STRING platform to construct a protein–protein interaction (PPI) network (Fig. 5C), and 53 core targets for ISO treatment of HS were obtained. In the PPI network, a node with a larger size and a greener color possesses a higher degree value. Of the identified

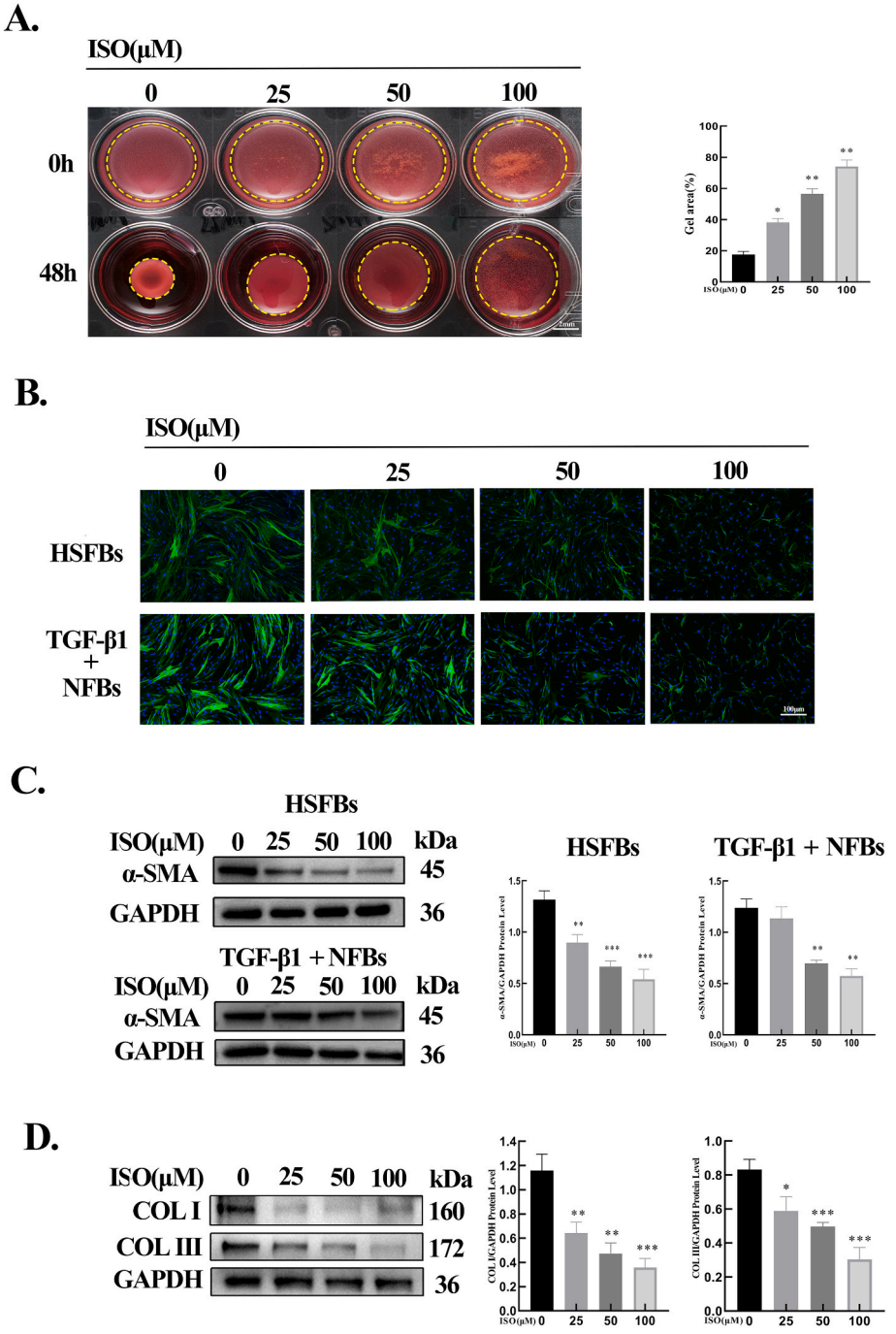

Fig. 4. ISO inhibited the gel contraction, myofibroblast activation, and collagen expression. A. Images and quantitative results of collagen gel contraction assay. Dotted lines indicated the gel areas. n = 3. B. Immunofluorescence staining of α-SMA in HSFBs and TGF-β1-stimulated NFBs. C. Western blotting results of α-SMA in HSFBs and TGF-β1-stimulated NFBs after treatment with ISO (0, 25, 50, 100 μM) for 48 h and the quantification of the protein levels normalized to GAPDH. D. Western blotting results of COL I and COL III in HSFBs and the quantification of COL I and COL III normalized to GAPDH. All assays were conducted with HSFBs after treatment with ISO of different concentrations (0, 25, 50, 100 μM) for 48 h. *$p < 0.05$, **$p < 0.01$, ***$p < 0.001$.

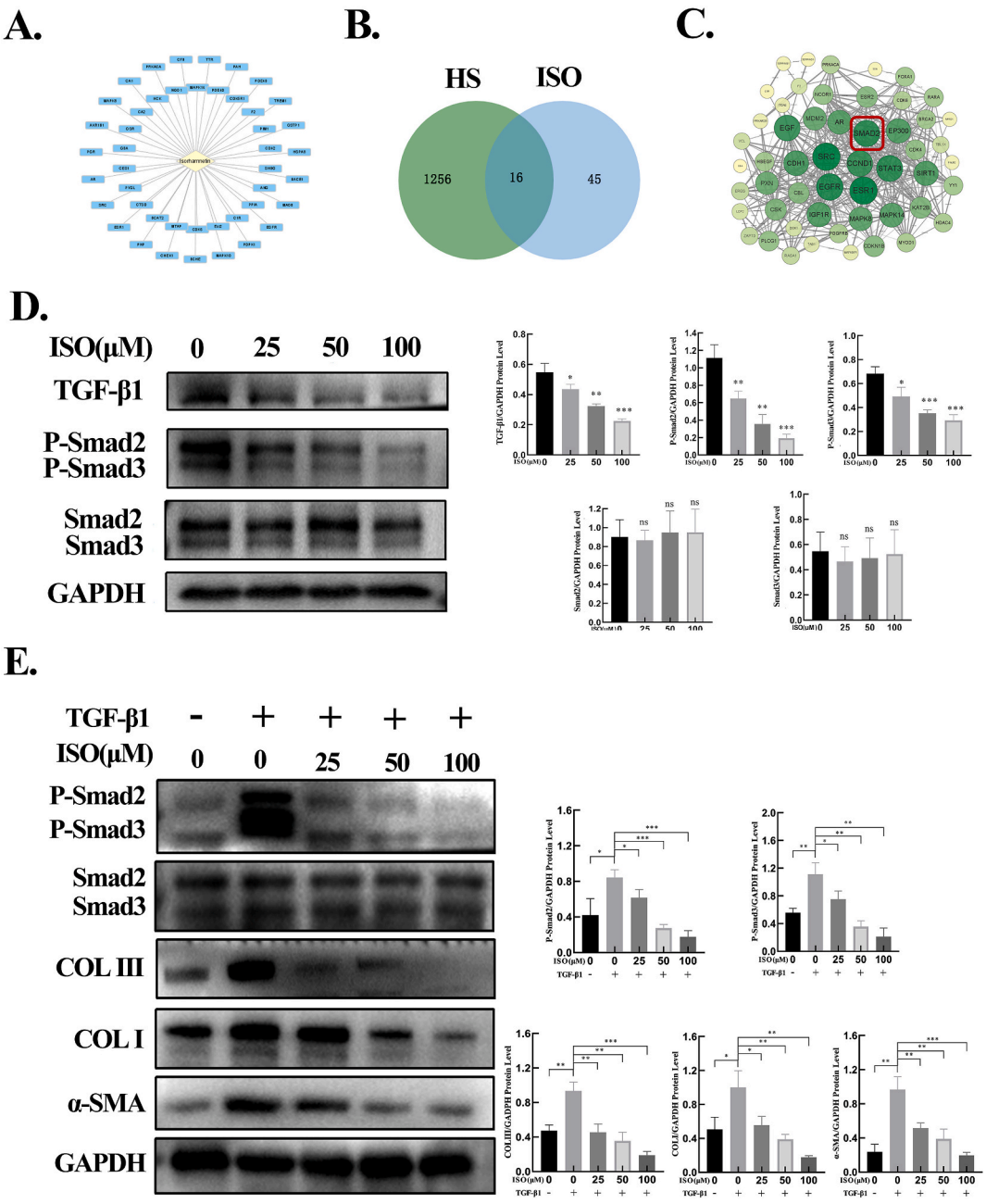

Fig. 5. ISO inhibited ECM production by suppressing the TGF-β1/Smad signaling pathway. A. Potential targets of ISO predicted by network pharmacology analysis. B. Intersection of ISO target genes and HS target genes. C. PPI network. D. The protein levels of TGF-β1, phosphorylated Smad2 and Smad3, and total Smad2 and Smad3 detected by western blotting and the quantification of protein levels normalized to GAPDH. E. The protein levels of phosphorylated and total Smad2/3, COL I, COL III, and α-SMA assessed by western blotting in HSFBs after treatment with ISO (0, 25, 50, 100 μM) + TGF-β1 (0, 10 ng/mL) for 48 h and the quantification of protein levels normalized to GAPDH. ns $p > 0.05$, *$p < 0.05$, **$p < 0.01$, ***$p < 0.001$.

ISO targets for HS treatment, TGF-β1 and Smad2 served as the key regulators via the TGF-β1/Smad signaling pathway.

6. ISO suppressed the TGF-β1/Smad signaling pathway in HFSBs

Based on the suppressive effects of ISO on HSFBs and the results of network pharmacology analysis, the protein expression of the TGF-β signaling pathway in HSFBs treated with ISO was determined using western blotting. Compared with the control group (0 μM), ISO treatment attenuated the protein levels of TGF-β1 as well as *p*-Smad2 and *p*-Smad3 in a dose-dependent manner. However, no

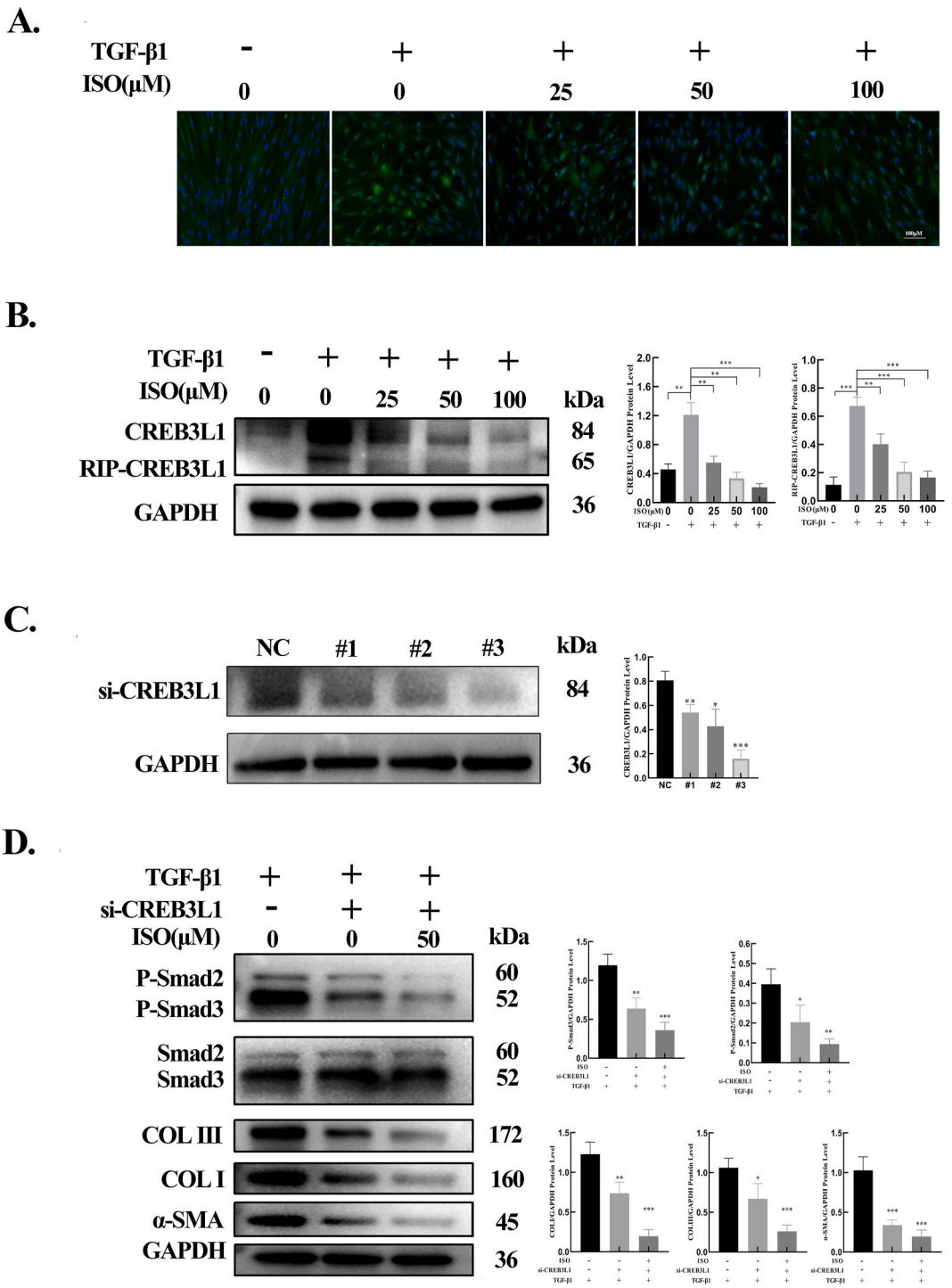

Fig. 6. ISO inhibited ECM production by suppressing the TGF-β1/CREB3L1 signaling pathway. A. Immunofluorescence staining of CREB3L1 in HSFBs after treatment with ISO (0, 25, 50, 100 μM) + TGF-β1 (0, 10 ng/mL) for 48 h. B. The protein levels of CREB3L1 and cleaved CREB3L1 detected by western blotting after HSFBs were treated with ISO (0, 25, 50, 100 μM) + TGF-β1 (0, 10 ng/mL) for 48 h, and the quantification of the protein levels normalized to the GAPDH level. C. The protein levels of CREB3L1 detected by western blotting after HSFBs were transfected with CREB3L1 siRNAs (si-CREB3L1#1, si-CREB3L1#2, and si-CREB3L1#3) and the quantification of the protein levels normalized to GAPDH. D. The protein levels of phosphorylated and total Smad2/3, COL I, COL III, and α-SMA in HFSBs treated with CREB3L1 siRNA or CREB3L1 siRNA combined with ISO (50 μM) for 48 h and the quantification of protein levels normalized to GAPDH. In this experiment, TGF-β1 (10 ng/mL) was added to induce the phosphorylation of Smad2/3 and the expression of COL I, COL III, and α-SMA. *$p < 0.05$, **$p < 0.01$, ***$p < 0.001$.

significant differences were observed in the protein levels of Smad2 and Smad3 (Fig. 5D). These results demonstrate that ISO ameliorated HS by downregulating TGF-β1 expression and the phosphorylation of Smad2 and Smad3.

7. ISO dose-dependently reduced the expressions of TGF-β1–induced α-SMA and collagen *in vitro*

Furthermore, the influence of ISO on TGF-β1–induced Smad2/3 phosphorylation and ECM production was examined. As illustrated in Fig. 5E, ISO treatment considerably attenuated the phosphorylation level of Smad2/3 stimulated by TGF-β1, but did not exert a substantial influence on the expression of total Smad2/3. Treatment with TGF-β1 alone significantly upregulated the protein levels of COL I, COL III, and α-SMA in the HSFBs relative to the control group. In contrast, ISO treatment significantly decreased the protein expressions of COL I, COL III, and α-SMA in the HSFBs induced by TGF-β1.

8. ISO inhibited RIP-mediated CREB3L1 cleavage via TGF-β1 signaling

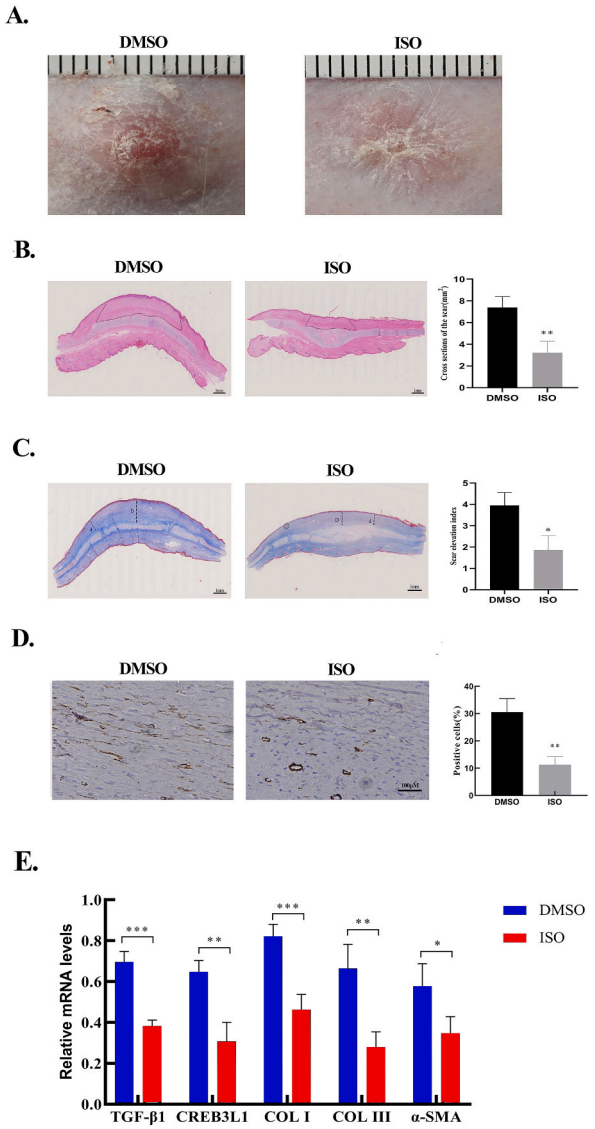

Fig. 7. ISO attenuated rabbit ear hypertrophic scar formation. A. The gross appearances of scars in the control group (treatment with DMSO) and the ISO group (treatment with 100 μM of ISO). B. H&E staining images and area quantification of cross-sections of hypertrophic scars from the control and ISO groups. Dotted lines indicate the scar areas. C. Masson Trichrome staining images and the quantification of SEI. The dotted lines "D" indicates the thickness of rabbit hypertrophic scars. The dotted lines "d" indicates the thickness of the adjacent normal skin. SEI is defined by the D/d ratio. D. Immunohistochemistry images of α-SMA from the DMSO and ISO groups. The quantification of the percentage of α-SMA-positive cells. E. The mRNA expression of TGF-β1, CREB3L1, COL I, COL III, and α-SMA in DMSO- and ISO-treated scar tissues detected by qRT-PCR and the quantification of the mRNA levels normalized to GAPDH. *$p < 0.05$, **$p < 0.01$, ***$p < 0.001$.

A previous study has confirmed that CREB3L1 can be cleaved into a transcription factor after TGF-β1 stimulation via RIP, which is then transferred to the nucleus and plays a role in the transcription of genes related to ECM synthesis [8]. To determine the potential effect of ISO on TGF-β1–induced CREB3L1 cleavage in HSFBs, different concentrations of both TGF-β1 and ISO were applied. The results of immunofluorescence staining indicated that TGF-β1 stimulation promoted the cleavage of CREB3L1 to an active transcription factor and its nuclear translocation, whereas ISO inhibited these processes (Fig. 6A). The results of western blotting indicated that treatment with TGF-β1 alone significantly upregulated the protein levels of CRB3L1 and cleaved CREB3L1 in the HSFBs relative to the control group. However, ISO significantly decreased the protein levels of cleaved CREB3L1 in HSFBs compared with TGF-β1 alone (Fig. 6B).

9. CREB3L1 silencing combined with ISO treatment further inhibited the expressions of proteins induced by TGF-β1

To investigate the effects of CREB3L1 on TGF-β1–induced protein expression, three CREB3L1 siRNAs (si-CREB3L1#1, si-CREB3L1#2, and si-CREB3L1#3) were transfected into HSFBs. As depicted in Fig. 6C, all siRNAs significantly knocked down CREB3L1 expression. As si-CREB3L1#3 exhibited the highest knockdown efficiency, it was selected for further studies. The results showed that CREB3L1 knockdown significantly decreased the protein levels of phosphorylated Smad2/3, α-SMA, COL I, and COL III. The combined treatment of CREB3L1 knockdown and ISO application resulted in a more pronounced inhibition of the expressions of phosphorylated Smad2/3, α-SMA, COL I, and COL III (Fig. 6D).

10. ISO attenuated rabbit ear HS formation

To ascertain the therapeutic effect of ISO *in vivo*, a rabbit ear HS model was established. At the gross level, compared with the control group (DMSO group), ISO treatment alleviated hyperemia and scar elevation, and the scars in the ISO-treated tissues were flatter and softer than those in the untreated tissues (Fig. 7A). Histologically, ISO treatment decreased the cross-sectional areas of the scars (Fig. 7B) as well as the SEI (Fig. 7C). Furthermore, ISO treatment attenuated the collagen density and resulted in a more regular arrangement of collagen fibers in the scar (Fig. 7C). Consistent with immunohistochemical staining results, the number of α-SMA–-positive cells were significantly reduced in the ISO-treated group (Fig. 7D). At the molecular level, ISO treatment lowered the mRNA expressions of TGF-β1, CREB3L1, COL I, COL III, and α-SMA (Fig. 7E). These *in vivo* findings were consistent with the *in vitro* results, which confirmed that ISO significantly inhibited HS formation by downregulating the expressions of genes involved in ECM production.

4. Discussion

HS is a chronic fibrotic skin disease that usually occurs after surgery, trauma, burn, or inflammation. HS is associated with symptoms of pain, itching, and joint dysfunction, which substantially affect the physical and mental health of patients. Although various therapeutic strategies are available for HS, their effects tend to be limited and unsatisfactory [19,20], and no drug can ideally solve this problem. Therefore, there is an urgent need to explore novel drugs to treat this condition. In this study, the potential of ISO to treat HS was investigated, and the findings revealed that ISO may serve as a novel candidate anti-HS drug. *In vitro* studies showed that ISO treatment suppressed the proliferation, migration, contractile ability of HFSBs, attenuated the expressions of COL I, COL III, and α-SMA, and inhibited TGF-β1–induced activation of HSFBs by reducing the levels of phosphorylated Smad2/3 and cleaved CREB3L1 in a dose-dependent manner. Moreover, ISO inhibited HSFBs by promoting cell apoptosis and cell cycle arrest in the G2 phase by upregulating the expressions of apoptosis-related proteins. In *in vivo* studies, ISO ameliorated HS formation in the rabbit ear HS model, which agreed with the results of *in vitro* experiments.

TGF-β is a multifunctional growth factor widely implicated in fibroblast proliferation, activation, and ECM production during HS formation [21]. During wound healing, TGF-β1 binds to its specific receptors and triggers the phosphorylation of Smad2/3. Subsequently, it interacts with Smad4 to form a transcriptional complex, which is translocated to the nucleus, binds to transcriptional coactivators or corepressors, and results in the overproduction of ECM and subsequent fibrosis [22]. Therefore, the TGF-β/Smad signaling pathway is a potential molecular target to regulate HS formation. In this study, network pharmacological analysis signified that ISO exerted an anti-HS effect by inhibiting the TGF-β/Smad signaling pathway. Western blot assay results showed that ISO downregulated TGF-β1. Furthermore, ISO suppressed the phosphorylation of Smad2 and Smad3, whereas the protein levels of total Smad2 and Smad3 remained unchanged. These findings imply that ISO suppresses the TGF-β/Smad pathway by dampening the expression of TGF-β1. These observations are in line with a previous study that reported the ability of ISO to attenuate liver fibrosis by inhibiting TGF-β/Smad signaling [11].

The signal transduction of the TGF-β/Smad pathway is extremely complex [23]. TGF-β–mediated collagen production is critically dependent on the phosphorylation of Smad2 and Smad3. However, this dependence applies only to the acute induction of collagen synthesis by TGF-β as the levels of phosphorylated Smad2/3 decrease within hours even if TGF-β1 persists. On the contrary, the collagen-stimulating effect of TGF-β1 can last for several days [6]. HS is a chronic fibrotic disease that depends on the long-term accumulation of collagens. Therefore, examining the key mechanism by which TGF-β1 induces the long-term accumulation of ECM is crucial to inhibiting HS formation. CREB3L1 is a transcription factor that belongs to the CREB/ATF family considered a transmembrane precursor in the endoplasmic reticulum [24]. CREB3L1 can be activated via cleavage mediated by site-1 protease and site-2 protease during the process of RIP [25]. These cleavages release the NH_2-terminal domain of the protein from the membranes, thus facilitating its entry into the nucleus, where it drives the transcription of genes needed for collagen assembly [26–28]. Recently, the

integrated analysis of single-cell and bulk transcriptome data revealed that CREB3L1 may function as a critical transcription factor in the myofibroblast of HS [29]. Previous studies have shown that TGF-β stimulates the proteolytic activation of CREB3L1, which is required for long-term collagen accumulation [8]. Other studies have shown that CREB3L1 contributes to the modification of myofibroblast phenotype via TGF-β1–mediated Smad-dependent canonical signaling, which ameliorates kidney fibrosis [30]. However, to the best of our knowledge, the significance of CREB3L1 in HS has so far not been explored. Initially, this study proved that the expression of RIP-CREB3L1 in HS tissues was significantly higher than that in NS tissues. Moreover, this work asserted that TGF-β1 stimulated the RIP of CREB3L1 in HSFBs. In addition, the phosphorylation levels of Smad2/3 and target genes, such as COL I, COL III, and α-SMA, increased under TGF-β1 stimulation. However, ISO reversed the increase in protein expression stimulated by TGF-β1. Interestingly, silencing CREB3L1 attenuated the phosphorylation of Smad2/3 and ECM deposition stimulated by TGF-β1. Also, the addition of ISO enhanced the effects of CREB3L1 silencing on the phosphorylation of Smad2/3 and ECM deposition. These findings signify that ISO inhibits TGF-β/Smad and TGF-β/CREB3L1 signaling pathways to achieve long-term inhibition of ECM synthesis. However, ISO is a botanical compound with multiple targets, which may further affect ECM synthesis in other ways.

This is the first study to demonstrate the involvement of CREB3L1 in the development of HS. Furthermore, this research has highlighted the stimulatory effects of TGF-β on the RIP of CREB3L1, which is required for long-term ECM synthesis. In addition, ISO inhibits HS formation by attenuating the RIP of CREB3L1 and dampening the TGF-β/Smad2/3 pathway. However, there are certain limitations in this work, which should be addressed. First, the exact molecules directly targeted by ISO remain elusive. Second, the precise mechanisms by which ISO suppresses the TGF-β/CREB3L1 pathway require further investigations. Third, the biosafety of ISO for potential clinical applications deserves in-depth studies.

5. Conclusions

Our data indicate that ISO suppresses HS formation by inhibiting the proliferation and migration of HSFBs, triggering their cell cycle arrest, and promoting their apoptosis. Moreover, ISO can affect the synthesis of ECM and the activation of HSFBs by downregulating the protein levels of TGF-β1, thus lowering the RIP of CREB3L1 and the phosphorylation of Smad2/3. Collectively, these results suggest that ISO is a promising anti-HS agent and an inhibitor of the TGF-β1–mediated CREB3L1/Smad signaling pathway.

Ethics approval and consent to participate

This study was reviewed and approved by the Institutional Review Board of the Xijing Hospital with the approval number: KY20233252-1, dated [7 March 2023]. All participants provided their written informed consents.

All animal experiments were approved by the Animal Investigation Committee of the Institute of Biomedical Sciences, the Fourth Military Medical University (license number: IACUC-20230031).

Funding

This research was funded by the National Natural Science Foundation of China (grant numbers: 82372530 and 82072182) and Shaanxi Provincial Science Foundation (grant number: 2020SF-179).

Informed Consent Statement: Informed consent was obtained from all subjects involved in the study.

Data availability statement

Data will be made available on request.

CRediT authorship contribution statement

Junzheng Wu: Writing – original draft, Validation, Project administration, Methodology, Investigation, Formal analysis. **Yajuan Song:** Writing – review & editing, Validation, Methodology, Formal analysis. **Jianzhang Wang:** Writing – review & editing, Validation, Methodology. **Tong Wang:** Writing – review & editing, Investigation. **Liu Yang:** Writing – review & editing, Supervision, Formal analysis. **Yi Shi:** Writing – review & editing, Supervision, Resources. **Baoqiang Song:** Writing – review & editing, Validation, Project administration, Methodology, Funding acquisition. **Zhou Yu:** Writing – review & editing, Validation, Project administration, Methodology, Funding acquisition, Data curation.

Declaration of competing interest

The authors declare the following financial interests/personal relationships which may be considered as potential competing interests:Baoqiang Song reports that financial support was provided by National Natural Science Foundation of China. Baoqiang Song reports that financial support was provided by Shaanxi Provincial Science Foundation.

Appendix A. Supplementary data

Supplementary data to this article can be found online at https://doi.org/10.1016/j.heliyon.2024.e33802.

References

[1] K. Lv, Z. Xia, Chinese expert consensus on clinical prevention and treatment of scar, Burns Trauma 6 (2018) 27, https://doi.org/10.1186/s41038-018-0129-9.
[2] E.E. Obi, Surgical considerations in skin of colour: minimizing pathological scars, Clin. Exp. Dermatol. 47 (8) (2022) 1429–1437, https://doi.org/10.1111/ced.15147.
[3] F.S. Frech, L. Hernandez, R. Urbonas, G.A. Zaken, I. Dreyfuss, K. Nouri, Hypertrophic scars and keloids: advances in treatment and review of established therapies, Am. J. Clin. Dermatol. 24 (2) (2023) 225–245, https://doi.org/10.1007/s40257-022-00744-6.
[4] D. Kiritsi, A. Nystrom, The role of TGFβ in wound healing pathologies, Mech. Ageing Dev. 172 (2018) 51–58, https://doi.org/10.1016/j.mad.2017.11.004.
[5] D. Peng, M. Fu, M. Wang, Y. Wei, X. Wei, Targeting TGF-β signal transduction for fibrosis and cancer therapy, Mol. Cancer 21 (1) (2022) 104, https://doi.org/10.1186/s12943-022-01569-x.
[6] J. Massague, TGFβ signalling in context, Nat. Rev. Mol. Cell Biol. 13 (10) (2012) 616–630, https://doi.org/10.1038/nrm3434.
[7] S. Aashaq, A. Batool, S.A. Mir, M.A. Beigh, K.I. Andrabi, Z.A. Shah, TGF-β signaling: a recap of SMAD-independent and SMAD-dependent pathways, J. Cell. Physiol. 237 (1) (2022) 59–85, https://doi.org/10.1002/jcp.30529.
[8] Q. Chen, C.E. Lee, B. Denard, J. Ye, Sustained induction of collagen synthesis by TGF-β requires regulated intramembrane proteolysis of CREB3L1, PLoS One 9 (10) (2014) e108528, https://doi.org/10.1371/journal.pone.0108528.
[9] G. Gong, Y.Y. Guan, Z.L. Zhang, et al., Isorhamnetin: a review of pharmacological effects, Biomed. Pharmacother. 128 (2020) 110301, https://doi.org/10.1016/j.biopha.2020.110301.
[10] J. Lei, J. Yang, C. Bao, et al., Isorhamnetin: what is the in vitro evidence for its antitumor potential and beyond? Front. Pharmacol. 15 (2024) 1309178 https://doi.org/10.3389/fphar.2024.1309178.
[11] N. Liu, J. Feng, X. Lu, et al., Isorhamnetin inhibits liver fibrosis by reducing autophagy and inhibiting extracellular matrix formation via the TGF-β1/smad3 and TGF-β1/p38 MAPK pathways, Mediat. Inflamm. (2019) 6175091, https://doi.org/10.1155/2019/6175091, 2019.
[12] J.H. Yang, S.C. Kim, K.M. Kim, et al., Isorhamnetin attenuates liver fibrosis by inhibiting TGF-β/Smad signaling and relieving oxidative stress, Eur. J. Pharmacol. 783 (2016) 92–102, https://doi.org/10.1016/j.ejphar.2016.04.042.
[13] T. Zhang, X.F. Wang, Z.C. Wang, et al., Current potential therapeutic strategies targeting the TGF-β/Smad signaling pathway to attenuate keloid and hypertrophic scar formation, Biomed. Pharmacother. 129 (2020) 110287, https://doi.org/10.1016/j.biopha.2020.110287.
[14] Y. Li, Z. Yu, D. Zhao, D. Han, Corilagin alleviates hypertrophic scars via inhibiting the transforming growth factor (TGF)-β/Smad signal pathway, Life Sci. 277 (2021) 119483, https://doi.org/10.1016/j.lfs.2021.119483.
[15] Q. Liang, F. Pan, H. Qiu, et al., CLC-3 regulates TGF-β/smad signaling pathway to inhibit the process of fibrosis in hypertrophic scar, Heliyon 10 (3) (2024) e24984, https://doi.org/10.1016/j.heliyon.2024.e24984.
[16] Y. Song, Z. Yu, B. Song, et al., Usnic acid inhibits hypertrophic scarring in a rabbit ear model by sup-pressing scar tissue angiogenesis, Biomed. Pharmacother. 108 (2018) 524–530, https://doi.org/10.1016/j.biopha.2018.06.176.
[17] X. Wu, Z. Wang, G. Wu, et al., Tetramethylpyrazine induces apoptosis and inhibits proliferation of hypertrophic scar-derived fibroblasts via inhibiting the phosphorylation of AKT, Front. Pharmacol. 11 (2020) 602, https://doi.org/10.3389/fphar.2020.00602.
[18] K. Vermeulen, Z.N. Berneman, D.R. Van Bockstaele, Cell cycle and apoptosis, Cell Prolif. 36 (3) (2003) 165–175, https://doi.org/10.1046/j.1365-2184.2003.00267.x.
[19] R. Ogawa, The most current algorithms for the treatment and prevention of hypertrophic scars and keloids: a 2020 update of the algorithms published 10 years ago, Plast. Reconstr. Surg. 149 (1) (2022) 79e–94e, https://doi.org/10.1097/PRS.0000000000008667.
[20] F.B. Rabello, C.D. Souza, J.J. Farina, Update on hypertrophic scar treatment, Clinics 69 (8) (2014) 565–573, https://doi.org/10.6061/clinics/2014(08)11.
[21] D. Avery, P. Govindaraju, M. Jacob, L. Todd, J. Monslow, E. Pure, Extracellular matrix directs phenotypic heterogeneity of activated fibroblasts, Matrix Biol. 67 (2018) 90–106, https://doi.org/10.1016/j.matbio.2017.12.003.
[22] X.M. Meng, D.J. Nikolic-Paterson, H.Y. Lan, Tgf-beta: the master regulator of fibrosis, Nat. Rev. Nephrol. 12 (6) (2016) 325–338, https://doi.org/10.1038/nrneph.2016.48.
[23] K. Luo, Signaling cross talk between tgf-β/smad and other signaling pathways, Cold Spring Harbor Perspect. Biol. 9 (1) (2017), https://doi.org/10.1101/cshperspect.a022137.
[24] Y. Zhao, Z. Yu, Y. Song, et al., The regulatory network of creb3l1 and its roles in physiological and pathological conditions, Int. J. Med. Sci. 21 (1) (2024) 123–136, https://doi.org/10.7150/ijms.90189.
[25] L. Sampieri, P. Di Giusto, C. Alvarez, Creb3 transcription factors: er-golgi stress transducers as hubs for cellular homeostasis, Front. Cell Dev. Biol. 7 (2019) 123, https://doi.org/10.3389/fcell.2019.00123.
[26] K. Andersson, B. Malmgren, E. Astrom, A. Nordgren, F. Taylan, G. Dahllof, Mutations in col1a1/a2 and creb3l1 are associated with oligodontia in osteogenesis imperfecta, Orphanet J. Rare Dis. 15 (1) (2020) 80, https://doi.org/10.1186/s13023-020-01361-4.
[27] Q. Chen, B. Denard, C.E. Lee, S. Han, J.S. Ye, J. Ye, Inverting the topology of a transmembrane protein by regulating the translocation of the first transmembrane helix, Mol. Cell 63 (4) (2016) 567–578, https://doi.org/10.1016/j.molcel.2016.06.032.
[28] A. Saito, I. Omura, K. Imaizumi, Creb3l1/oasis: cell cycle regulator and tumor suppressor, FEBS J. (2024), https://doi.org/10.1111/febs.17052.
[29] S. Zhang, Y. Zhang, P. Min, Single-cell and bulk transcriptome data integration reveals dysfunctional cell types and aberrantly expressed genes in hypertrophic scar, Front. Genet. 12 (2021) 806740, https://doi.org/10.3389/fgene.2021.806740.
[30] Y. Miyake, M. Obana, A. Yamamoto, et al., Upregulation of oasis/creb3l1 in podocytes contributes to the disturbance of kidney homeostasis, Commun. Biol. 5 (1) (2022) 734, https://doi.org/10.1038/s42003-022-03709-x.